A spatial truncation approach to the analysis of optical imaging of the retina in humans and cats

Michael D. Abramoff[1], MD, PhD (Member IEEE), Young H. Kwon[1], MD, PhD, Dan Ts'o[2], PhD, Hongbin Li, MD, PhD[2], Simone Berriga[3], Peter Soliz[3], PhD, Randy Kardon[1], MD, PhD

(1) Department of Ophthalmology and Visual Sciences, University of Iowa Hospitals and Clinics, 200 Hawkins Drive, Iowa City, IA 52242, USA. (2) Department of Neurosurgery, SUNY Health Sciences Center, 750 East Adams St, Syracuse, NY 13210, USA. (3) Kestrel co., 3815 Osuna NE, Albuquerque, NM 87109, USA.

Purpose

Optical imaging of the retina is a new means for imaging retinal function and has been demonstrated in pilot studies of anesthetized cats and monkeys, as well as awake humans [1;2]. The retinal optical imaging signal is a very small and complex signal, with an amplitude of typically 0.1% or less of total retinal reflectance. It is an indirect measure of retinal neural activity, where the reflectance to light of a specific wavelength changes as a result of visual stimulation [3]. Typically 2000-3000 images are obtained during different visual stimulus conditions. Because of the weakness of the signal, extraction of the 'true' retinal response is a formidable task. For the brain cortex, optical imaging is well studied [4], and sophisticated image analysis methods have been developed to reduce the considerable variations in signal intensity not due to the stimulus, but to causes such as breathing, heartbeat, camera motion, camera temperature instability and others. These methods include principal component analysis (PCA) [5], and extensions thereof, such as truncated differencing, Infomax [6] and extended spatial decorrelation [7]. It therefore seems natural to employ these methods for analysis of retinal optical imaging also. Nevertheless, important differences exist: first, the images are obtained through the pupil in awake humans, so that saccadic eye movements and the coupling of the optics of the camera and the eye cause a major source of noise ("vignetting") [8]; this issue is aggravated because the eye movements can be time-locked to the stimulus when the subject reacts to the sudden appearance of a stimulus; and in awake humans there is much larger variation in the optical imaging signal due to 'vasomotion' than in anesthetized animals with controlled breathing [9]. Additionally, the time-course of the impulse response of the retinal optical imaging signal is not well established, while the above methods often use this time-course as a constraint [10;11]. On the other hand, the spatial distribution of the signal is expected to closely resemble the spatial distribution of the projection of the stimulus. Finally, optical imaging of the retina is still in its early infancy, necessitating algorithms that can analyze data quickly, so that experimental conditions can be adjusted without having to wait a long period of time for results. The purpose of this paper is to describe an extension of the above methods using the expected spatial distribution of the retinal optical imaging signal as a constraint, meanwhile discarding any assumptions about the temporal distribution of the signal.

Subjects and Data Collection

Retinal optical imaging was performed in humans and cats. Techniques for animal preparation and image acquisition in cats have been presented elsewhere [1]. In humans, four subjects were studied using optical imaging device (OID, manufactured by Kestrel inc., Albuquerque, NM) to obtain sequences of retinal reflectance images. The research adhered to the tenets of the declaration of Helsinki. The "interrogation" light was used to illuminate the retina at 780 nm bandwidth, and the reflected light recorded by a 12-bit electrothermally cooled CCD camera with a frame size of 264x256 pixels at 12-bit resolution. The visual stimulus is generated by an integrated computer board and displayed on a LCD screen integrated into the optical pathway of the OID. Placed in front of this screen is a 550nm 24nm bandwidth filter to let through the stimulus only. Stimuli are counterflickering squares with a spatial frequency of about 0.5cycles per degree, projected either as two squares diagonally opposite the fixation point ("butterfly" or DIAG stimulus, see Figure 1), or vertical and horizontal bars of about 20º x 5º projected approximately 10º from the fixation. Commonly, a minimum of 30-40 runs ("epochs") are acquired, each consisting of 50-110 image frames at 10 Hz, approximately 1 Gbytes of data.

Analysis methods

Each experiment is represented as T images of the retina recorded by the OID, collected at times $t \in 0...T$, while the intensity of a pixel $\boldsymbol{r} = (x, y) \in P_{x,y}$ in the t-th image, as recorded by the camera, is $f_o(\boldsymbol{r}, t)$. The images are registered to correct for eye-movements using a mutual information based registration algorithm [12] correcting for translation and rotation only, smoothed with a Gaussian kernel at scales σ and mean subtracted

0-7803-8388-5/04/$20.00 ©2004 IEEE

to obtain $f_\sigma(\mathbf{r},t) = f_o(\mathbf{r},t) - \frac{1}{T}\sum_t f_o(\mathbf{r},t)$. *f* can then be rewritten as a linear combination of principal components $\psi_n(\boldsymbol{r})$ as follows:

$$f_\sigma(\mathbf{r},t) = \sum_n a_n(t)\psi_n(\mathbf{r}) \qquad (1)$$

where the principal components $\psi_n(\boldsymbol{r})$, are the eigenvectors from

$$\psi_n C = \psi_n \lambda_n$$

with *C* the image-wise (spatial) covariance matrix of *f*, $C(\mathbf{x},\mathbf{y}) = \frac{1}{N}\sum_t f_\sigma(\mathbf{x},t) f_\sigma(\mathbf{y},t)$, the coordinates a_n, the projection of each $f_\sigma(t)$ onto $a_n(t) = \sum_{\mathbf{r}} f_\sigma(\mathbf{r},t)\psi_n(\mathbf{r})$, and the ψ_n ordered by descending value of their eigenvalue λ_n,(the square of the variance of ψ_n), so that the components that explain most of the variance of *f* come first.

Trivially, the whole data set *f* can be easily reconstituted from the coordinates and components as in (1), but by including only a subset of the components $\psi_n, a_n, n \in S$ and then reconstituting as follows

$$f_{\sigma,s}(\mathbf{r},t) = \sum_{n\in S} a_n(t)\psi_n(\mathbf{r})$$

different constraints can be placed on the 'cleaned' $f_{\sigma,s}$. Such constraints can be of varying complexity and in the literature include a bound on the confidence in the correlation of the coordinates a_n with the time-course of the stimulus, a method called truncated differencing [10], a bound on the signal-to-noise-ratio and signal power, called generalized indicator function [11], and constraints on the smoothness and uncorrelatedness of signal sources, called extended spatial decorrelation [7]. As discussed above, in optical imaging of the retina it is reasonable to assume that the spatial distribution of the signal will be similar to the spatial distribution of the projection of the stimulus. Therefore statistical significance testing is applied to the $\psi_n, n \in S$, using the correlation with the *stimulus image* at at the same scale σ, $f_{\sigma,c}(\mathbf{x})$, as a basis:

$$f_{\sigma,c}(\mathbf{x}) = \begin{cases} 1 \text{ if the retina was stimulated at } \mathbf{x} \\ 0 \text{ if the retina was not stimulated at } \mathbf{x} \end{cases}$$

with the correlation $r_n(f_c,\psi_n)$ defined as

$$r_n(f_c,\psi_n) = \frac{\sum_r \psi_n(\boldsymbol{r}) f_c(\boldsymbol{r})}{\|\psi_n\|\|f_c\|} \qquad (4)$$

and the probability of observing a correlation whose absolute value is larger than r_n defined as

$$\overline{P_n} = erf\left(\sqrt{\frac{N}{2}}|r_n|\right) \qquad (5)$$

By computing the linear combination of those $\psi_n, n \in S$ constrained by $\overline{P_n} > 0.95$, over a range of scales σ, a spatial truncation map $f_{\sigma,s}$ is obtained that contains the components that most closely resemble the spatial distribution of the visual stimulus $f_c(\boldsymbol{x})$ at scale σ, for which the timecourse can then be obtained from the a_n.

Results

For this study, the range of σ was between 1 to 25 pixels. Figure 2 shows the fraction of variance that is related to the time-courses of the stimulus, the x- and the y-movement respectively. The x- and y-movement time-courses

are the translation parameters for individual $f_o(\boldsymbol{r}, t)$ found by the registration analysis. It can be seen that in nearly all studies, the signal variance timelocked to the stimulus is at least as large as that timelocked to the stimulus. Figure 3 displays the first principal component of the f_s spatial truncation maps for four different horizontal and vertical bar stimulus conditions in the cat and for two different stimulus conditions in a human subject, at scale 20 respectively 10 pixels. In the other human subjects similar maps could be obtained though the variation in time-course is large. Figure 4 shows the time course for all stimulus conditions shown in Figure 3.

Discussion

We have proposed a new method for the extraction of the retinal optical imaging signal in humans and cats, based on the assumption that in the retina the spatial distribution of the signal is similar to that of the projection of the visual stimulus. The obtained spatial truncation maps, though noisy, have time-courses that may fit the known physiologyl. One of the reasons for developing a new method was that the results of analysis using truncated differencing and extended spatial decorrelation appeared non-optimal, possibly due to the . One important reason for this may be the large amount of motion in the retinal optical image sequences [R. Schiessl, personal communication] as shown in Figure 1, where the variance due to x- and y-motion of the eye is at least as large as all variance that is stimulus time-locked (which as explained above also includes movement). The problem with eye movements is that they do not only make pixel-to-pixel comparisons difficult, because of the non-linear relationship between the optical axis of the optical system created by the camera and the optics of the eye, but also because the eye rotation that shows up as image motion causes a change in the angle of incidence of the interrogation light, so that the reflectance changes due to the movement are difficult to separate from activity related reflectance changes. Additionally, when the stimulus suddenly appears somewhere in the visual field, most subjects find it difficult to suppress the urge to fixate the stimulus, so that the movement is also partially locked in time to the stimulus. In view of these significant sources of noise, and many others not discussed in this paper, in our opinion it is encouraging that a retinal optical imaging signal can be shown in humans with a time course that seems physiological. Of course, the assumption that the retinal optical imaging response is similar in shape to the stimulus has to be investigated more fully. We are currently comparing the results obtained by spatial truncation to other methods, including independent component analysis and generalized indicator functions[11], and we hope to give a more quantitative comparison of these methods in the future. In summary, we have shown that spatial truncation shows promise for the analysis of retinal optical imaging.

Figures

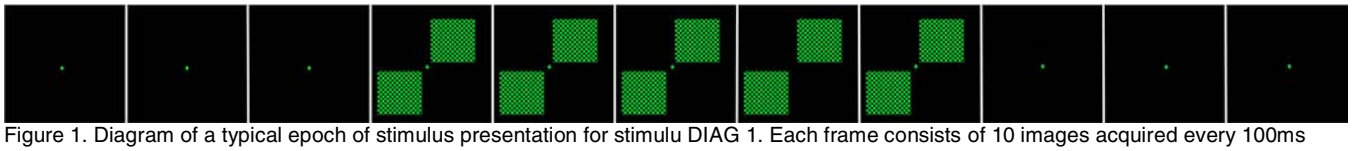

Figure 1. Diagram of a typical epoch of stimulus presentation for stimulu DIAG 1. Each frame consists of 10 images acquired every 100ms (10Hz frame rate): 3s (30 frames) pre-stimulus frames for the analysis baseline (blank stimulus screen), followed by 5s (50 frames) of a counterflickering checkerboard stimulus, in this case two squares diagonally opposite the fixation point, followed by 3s (30 frames) post-stimulus frames (again blank stimulus screen). A fixation light in the center is projected continuously during the whole epoch.

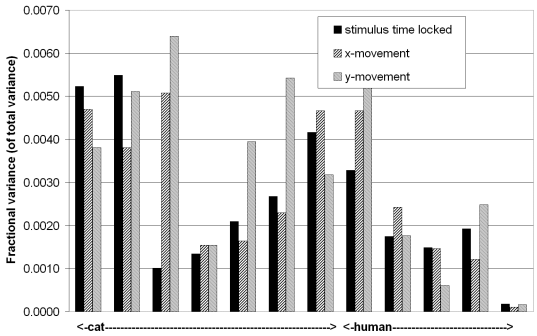

Figure 2. Fractional variance (as a fraction of total variance) explained by stimulus-time-locked events, x-movement and y-movement, for 7 studies in cats and 5 studies in humans, in chronological order.

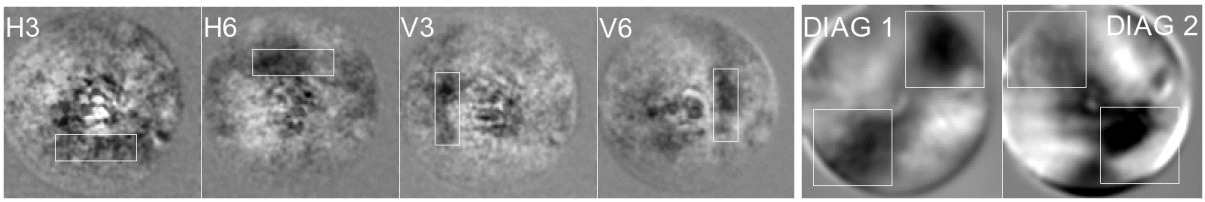

Figure 3. Spatial truncation maps of retinal optical imaging for (left), the cat and (right) human subject, at scale 20 pixels (left) and 10 pixels (right). The approximate stimulated areas are indicated in each image:H3, horizontal bar stimulus in upper visual field - H6, lower visual field, V3 - vertical bar in left visual field, V6 right visual field, DIAG 1 and DIAG 2, butterfly shaped stimulus as shown in Figure 1. Remember that the image on the retina is inverted! The noise in the center of the maps is probably related to the fixation light.

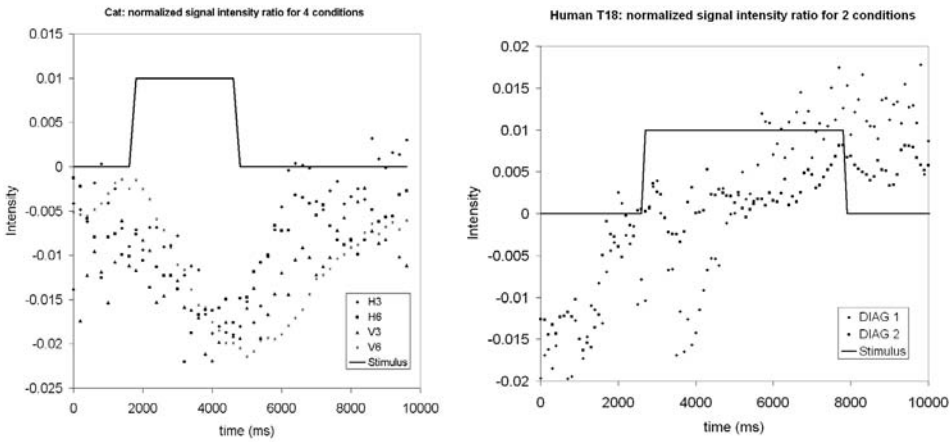

Figure 4. Time courses of the spatial truncation maps shown in Figure 3 (left) cat, (right) human. Vertical axis: fraction of total intensity (normalized), horizontal axis (time in ms). There is a large difference between the impulse responses in the cat and the human. This may be due to either the different spatial or temporal distribution of the stimuli, or the different metabolism of cat and human retina.

References

[1] Ts'o, D., Li, H., Kwon, Y. H., Truitt, P., and Soliz, P., "Intrinsic signal optical imaging of retinal responses to patterned stimuli," *Invest Ophthalm Vis Sci [ARVO abstract]*, vol. 43, no. 4, 2003.

[2] Kardon, R., Kwon, Y. H., Ts'o, D., and Soliz, P. Optical Imaging Device of Retinal Function. 4611-4640. 2002. The International Society of Optical Engineering, Photonics West, Ophthalmic technologies XII.
Ref Type: Conference Proceeding

[3] Cohen, L. B., "Changes in neuron structure during action potential propagation and synaptic transmission," *Physiol Rev.*, vol. 53, no. 2, pp. 373-418, Apr.1973.

[4] Ts'o, D. Y., Frostig, R. D., Lieke, E. E., and Grinvald, A., "Functional organization of primate visual cortex revealed by high resolution optical imaging," *Science*, vol. 249, no. 4967, pp. 417-420, July1990.

[5] Sirovich, L. and Kaplan, E., "Analysis methods for optical imaging," in Frostig, R. D. (ed.) *Methods for in vivo optical imaging of the central nervouse system* Boca Raton, FL: CRC Press, 2001.

[6] Bell, A. J. and Sejnowski, T. J., "An information-maximization approach to blind separation and blind deconvolution," *Neural Comput.*, vol. 7, no. 6, pp. 1129-1159, Nov.1995.

[7] Schiessl, I., Stetter, M., Mayhew, J. E., McLoughlin, N., Lund, J. S., and Obermayer, K., "Blind signal separation from optical imaging recordings with extended spatial decorrelation," *IEEE Trans.Biomed.Eng*, vol. 47, no. 5, pp. 573-577, May2000.

[8] Hoover, A. and Goldbaum, M., "Locating the optic nerve in a retinal image using the fuzzy convergence of the blood vessels," *IEEE Trans.Med.Imaging*, vol. 22, no. 8, pp. 951-958, Aug.2003.

[9] Shoham, D. and Grinvald, A., "The cortical representation of the hand in macaque and human area S-I: high resolution optical imaging," *J.Neurosci.*, vol. 21, no. 17, pp. 6820-6835, Sept.2001.

[10] Gabbay, M., Brennan, C., Kaplan, E., and Sirovich, L., "A principal components-based method for the detection of neuronal activity maps: application to optical imaging," *Neuroimage.*, vol. 11, no. 4, pp. 313-325, Apr.2000.

[11] Yokoo, T., Knight, B. W., and Sirovich, L., "An optimization approach to signal extraction from noisy multivariate data," *Neuroimage.*, vol. 14, no. 6, pp. 1309-1326, Dec.2001.

[12] Ritter, N., Owens, R., Cooper, J., Eikelboom, R. H., and van Saarloos, P. P., "Registration of stereo and temporal images of the retina," *IEEE Trans.Med.Imaging*, vol. 18, no. 5, pp. 404-418, May1999.